

# Structural and Kinetic Features of Family I Inorganic Pyrophosphatase from *Vibrio cholerae*

E. V. Rodina<sup>1,2\*</sup>, V. R. Samygina<sup>3</sup>, N. N. Vorobyeva<sup>1</sup>,  
T. S. Sitnik<sup>2</sup>, S. A. Kurilova<sup>2</sup>, and T. I. Nazarova<sup>2</sup>

<sup>1</sup>Chemistry Faculty, Lomonosov Moscow State University, 119992 Moscow, Russia;  
fax: (495) 932-8846; E-mail: rodina@belozersky.msu.ru

<sup>2</sup>Belozersky Institute of Physico-Chemical Biology, Lomonosov Moscow State University,  
119992 Moscow, Russia; fax: (495) 939-3181; E-mail: nazarova@belozersky.msu.ru

<sup>3</sup>Shubnikov Institute of Crystallography, Russian Academy of Sciences, Leninsky pr. 59,  
119333 Moscow, Russia; E-mail: lera@crys.ras.ru

Received December 23, 2008

Revision received February 12, 2009

**Abstract**—In this paper, kinetic properties of a soluble inorganic pyrophosphatase of family I from *Vibrio cholerae* (V-PPase), intestinal pathogen and causative agent of human cholera, are characterized in detail, and the crystal structure of a metal-free enzyme is reported. Hydrolytic activity of V-PPase has been studied as a function of pH, concentration of metal cofactors ( $Mg^{2+}$  or  $Mn^{2+}$ ), and ionic strength. It has been found that, despite the high conservation of amino acid sequences for the known bacterial PPases of family I, V-PPase differs from the other enzymes of the same family in a number of parameters. Dissociation constants of V-PPase complexed with  $Mg^{2+}$  or  $Mn^{2+}$  were essentially the same as for *Escherichia coli* PPase (E-PPase). However, the pH optimum of  $MgPP_i$  hydrolysis by V-PPase was shifted to more alkaline pH due to higher values of the  $pK_a$  of ionizable groups for both the free enzyme and the enzyme–substrate complex. The stability of a hexameric form of V-PPase has been studied as a function of pH. The corresponding  $pK_a$  of a group that controls the stability of the hexamer at pH below 6 ( $pK_a = 4.4$ ) was significantly lower than in the other hexameric PPases. The crystal structure reported here is analyzed and compared with the structure of E-PPase. The location of amino acid residues that differ in V-PPase and E-PPase is discussed. Since V-PPase has been found to retain its hydrolytic activity in high ionic strength media, the observed structural and kinetic features are analyzed in view of the possible osmoadaptation of this protein.

DOI: 10.1134/S0006297909070050

**Key words:** pyrophosphatase, *Vibrio cholerae*, osmoadaptation, X-ray analysis, crystal structure

*Vibrio cholerae* is a Gram-negative facultative anaerobe, an intestinal pathogen that causes cholera in humans. *Vibrio cholerae* occurs naturally in estuarine environments characterized typically by high salinity, mostly due to salts of sodium and potassium. *Vibrio cholerae* is a moderately halophilic organism. Its optimal growth requires supplementation with 5–15 mM NaCl and KCl, but it is capable of growth at NaCl concentration of 500 mM and higher [1, 2]. In response to increasing environmental osmolarity, halophilic bacteria activate ionic transport resulting in the elevation of intracellular concentration of  $K^+$  and  $Na^+$ . Along with this, nonionic osmolytes like sugars or amino acid derivatives are syn-

thesized in the cell to maintain osmotic equilibrium without excess of charged osmolytes like  $K^+$  and  $Na^+$ . Therefore, it is essential for growth that cytoplasmic proteins of *V. cholerae* can function in media with high concentration of monovalent cations and high osmolarity. For particular proteins of *V. cholerae*, little is known about mechanisms of their adaptation to changes in ionic composition or elevated ionic strength of the environment. However, general principles of this phenomenon are widely investigated [1–7]. Knowing the strategy of osmoadaptation of halophilic pathogens is of high practical interest because on this basis specific antibacterial agents can be developed.

Soluble inorganic pyrophosphatases (PPases) catalyze hydrolysis of pyrophosphate ( $PP_i$ ), which is formed in the course of a number of biosynthetic processes. These enzymes are found in all known organisms and are

**Abbreviations:** E-PPase, *Escherichia coli* inorganic pyrophosphatase; V-PPase, *Vibrio cholerae* inorganic pyrophosphatase.

\* To whom correspondence should be addressed.

absolutely necessary for cell growth and division [8]. On the basis of their structure and properties, PPases are divided into non-homologous families I and II. Family I includes all known eucaryotic and most bacterial PPases; PPases of family II found in some archaeobacteria and eubacteria are much less common enzymes. *Vibrio cholerae* is one of four unique species that have PPases of both families encoded in their genomes [9]. It has been shown earlier that both classes of PPases in *V. cholerae* can be expressed *in vitro* in the active form, catalytic parameters being typical for their corresponding families [10]. The object of this study is PPase of family I from *V. cholerae* (V-PPase). Its kinetic properties are investigated in detail in comparison with *E. coli* PPase, to which V-PPase has 84% sequence identity. Hydrolytic activity of V-PPase is studied as a function of pH, concentration of metal cofactors ( $Mg^{2+}$  and  $Mn^{2+}$ ), and salts of monovalent cations (NaCl, KCl, and  $NH_4Cl$ ). Stability of the most active, hexameric, form of V-PPase is investigated as a function of pH. The crystal structure of a metal-free form of V-PPase is solved and analyzed in comparison with the structure of E-PPase. Kinetic features of V-PPase are discussed on the basis of the structural data.

## MATERIALS AND METHODS

**Chemicals.** The chemicals used in the study were purchased in high-purity grade from Sigma (USA), Fluka (Switzerland), Serva (Germany), Merck (Germany), or Pharmacia Fine Chemicals (Sweden). All stock solutions were freshly prepared with deionized water additionally purified with a MilliQ apparatus.

**Isolation and purification of V-PPase.** Plasmid for expression of recombinant *V. cholerae* PPase was kindly provided by Prof. R. Lahti (Turku, Finland). V-PPase was expressed, isolated, and purified as described earlier for *Micobacterium tuberculosis* PPase [11]. At the last step of purification, V-PPase was eluted from a column with DEAE-Sepharose at 0.2 M NaCl. The yield of V-PPase was 126 mg from 3 liters of cell culture. The purity of the protein preparation as characterized by polyacrylamide gel electrophoresis was at least 98%.

**Kinetic measurements.** Hydrolytic activity of V-PPase was determined at 25°C by the rate of  $P_i$  release using a semi-automatic phosphate analyzer [12]. Total concentrations of  $MgCl_2$  and  $Na_4P_2O_7 \cdot 10 H_2O$  were calculated using the values of dissociation constants for  $MgPP_i$  and  $Mg_2PP_i$  calculated at different pH values as described in [13]. In the case of  $Mn^{2+}$ -supported hydrolysis at pH 7.5, 23  $\mu M$  and 0.13 mM were used for  $MnPP_i$  and  $Mn_2PP_i$ , respectively.

Kinetic parameters of  $Mg^{2+}$ -supported hydrolysis of  $PP_i$  were determined in 50 mM buffer (Mes-NaOH, pH 6.5; Hepes-NaOH, pH 7.5; or Tris-HCl, pH 9.0), at 2, 5, or 10 mM  $Mg^{2+}$  and 3–200  $\mu M$   $MgPP_i$ . Kinetic param-

eters of  $Mn^{2+}$ -supported hydrolysis of  $PP_i$  were determined in 50 mM Tris-HCl, pH 7.5, at 50  $\mu M$   $Mn^{2+}$  and 3–30  $\mu M$   $MnPP_i$ . The effect of NaCl, KCl, or  $NH_4Cl$  on the rate of hydrolysis of  $MgPP_i$  was studied in 50 mM Tris-HCl, pH 7.5, at 2 mM  $Mg^{2+}$  and 30  $\mu M$   $MgPP_i$ . Kinetic parameters as a function of pH were determined in 50 mM buffers (Mes-NaOH, pH 6.5–7.5; Hepes-NaOH, pH 7.0–8.3; Tris-HCl, pH 7.5–9.0; Capso-NaOH, pH 9.0–10.0; Caps-NaOH, pH 10.0–11.0) at 5 mM  $Mg^{2+}$ . Parameters of pH dependence were determined as the best fit of Eqs. (1a) and (1b) to the experimental data:

$$k^{app} = k_{cat}/(1 + [H^+]/K_{ESH_2} + K_{ESH}/[H^+]), \quad (1a)$$

$$k^{app}/K_m^{app} = (k_{cat}/K_m)/(1 + [H^+]/K_{EH_2} + K_{EH}/[H^+]), \quad (1b)$$

where  $k^{app}$  and  $k^{app}/K_m^{app}$  are apparent values of kinetic parameters at given pH;  $k_{cat}$  and  $k_{cat}/K_m$  are pH-independent values of kinetic parameters.

The rates of hydrolysis of  $PP_i$  as a function of metal cofactor concentration were measured in 50 mM Tris-HCl, pH 7.5, at 50  $\mu M$   $MgPP_i$  and 0.03–10 mM  $Mg^{2+}$  (for  $Mg^{2+}$ -supported hydrolysis), or at 20  $\mu M$   $MnPP_i$  and 1–300  $\mu M$   $Mn^{2+}$  (for  $Mn^{2+}$ -supported hydrolysis). Parameters of this dependence were determined as the best fit of Eq. (2) to the experimental data:

$$A = \frac{A_0 [M^{2+}]}{K_d(M2) + [M^{2+}] + [M^{2+}]^2/K_d(M4)}, \quad (2)$$

where  $[M^{2+}]$  is concentration of a metal cofactor;  $K_d(M2)$  and  $K_d(M4)$  are dissociation constants of the complexes enzyme–cofactor metal ion bound at site M2 or M4, respectively; and  $A_0$  is maximum level of enzyme activity without inhibition.

**Sedimentation analysis.** Velocity sedimentation of the solutions of V-PPase in 0.1 M buffers (Mes-NaOH, pH 3.0–5.5; Hepes-NaOH, pH 7.5; enzyme concentration 10–20  $\mu M$ ) was carried out at 20°C using a Spinco E analytical ultracentrifuge (Beckman, USA) (48,000 rpm, scanning at 280 nm). Sedimentation coefficient was calculated as the average from at least three independent experiments.

**Crystallization and data collection.** V-PPase crystals were grown for two weeks using the vapor diffusion technique from 0.1 M imidazole buffer, pH 8.0, containing 15–20% 2,4-methylpentanediol, and 3% PEG-4000. Protein concentration was 8–10 mg/ml. Colorless crystals of 0.1–0.2 mm were obtained. The X-ray diffraction data were collected at 100 K at DESY station (Germany) using synchrotron radiation at a wavelength of 1.05 Å and MAR-CCD detector (Marresearch, Germany). The complete data set was collected to a resolution limit of 2.0 Å. The crystal belonged to space group P3, parameters of the unit cell are  $a = b = 66.56$  Å,  $c = 66.2$  Å.

Completeness of the set was 95.8% (95.6%),  $R_{\text{merge}} = 7.1\%$  (48.0%),  $I/\text{sig}(I) = 10.0$  (2.0) (values in parentheses are given for the highest-resolution shell). The diffraction data were processed and scaled using the DENZO and SCALEPACK program packages [14].

**Structure refinement.** The structure of V-PPase was obtained by molecular replacement with the program MOLREP [15] using the structure of *E. coli* PPase (PDB ID 1auu [16]) as an initial model. V-PPase contained two monomers in the asymmetric part of the unit cell. The structure was refined with the program Refmac, v.5 [17], using isotropic refinement of the temperature factors, followed by additional correction with the Coot program [18]. The crystal structures were analyzed and aligned with the Coot program; alignment and analysis of the amino acid sequences were performed using the programs available online at the ExPaSy server (<http://au.expasy.org/> [19]).

## RESULTS AND DISCUSSION

**Kinetic parameters of PP<sub>i</sub> hydrolysis.** Kinetic parameters of hydrolysis of pyrophosphate by *V. cholerae* PPase were determined at several fixed pH values and concentrations of metal cofactors (Table 1). Dissociation constants  $K_d(\text{M2})$  were determined for the complexes of V-PPase with the most efficient metal cofactors,  $\text{Mg}^{2+}$  and  $\text{Mn}^{2+}$  (Table 2). The pH dependence of kinetic parameters of  $\text{Mg}^{2+}$ -supported hydrolysis of PP<sub>i</sub> was studied, and the  $\text{p}K_a$  values were determined for the catalytic groups of free enzyme ( $\text{p}K_{\text{EH}_2}$  and  $\text{p}K_{\text{EH}}$ ) and enzyme–substrate complex ( $\text{p}K_{\text{ESH}_2}$  and  $\text{p}K_{\text{ESH}}$ , Table 3).

Analysis of the parameters obtained here for V-PPase compared to analogous parameters of E-PPase demonstrates that, despite the high similarity of their amino acid sequences, these two enzymes do not show identical kinetic behavior. One example of this difference is revealed upon the analysis of their interaction with metal cofactors  $\text{Mg}^{2+}$  and  $\text{Mn}^{2+}$ . The active site of PPase is capable of binding a total of four metal ions. Two of them have to occupy activator sites M1 and M2 prior to sub-

**Table 1.** Kinetic parameters of hydrolysis of PP<sub>i</sub> by *V. cholerae* PPase

Conditions	$K_m$ , $\mu\text{M}$	$k_{\text{cat}}$ , $\text{sec}^{-1}$
pH 7.5, 2 mM $\text{Mg}^{2+}$	$4.0 \pm 0.5$	$93 \pm 3$
pH 7.5, 50 $\mu\text{M}$ $\text{Mn}^{2+}$	$2.8 \pm 0.2$	$51 \pm 2$
pH 9.0, 5 mM $\text{Mg}^{2+}$	$2.6 \pm 0.2$	$177 \pm 3$
pH 6.5, 10 mM $\text{Mg}^{2+}$	$7 \pm 1$	$38 \pm 2$

strate binding in order to bring the enzyme to a catalytically competent state. The site M3 is occupied by a metal ion that is bound as a part of a substrate molecule ( $\text{MgPP}_i$  or  $\text{MnPP}_i$ ). Occupation of the site M4 is known to cause inhibition of the other family I PPases [13]. Affinity of PPase for metal cofactors at sites M1 and M3 cannot be determined from kinetic data. Dissociation constants of PPase complexed with  $\text{Mg}^{2+}$  or  $\text{Mn}^{2+}$  at sites M2 and M4 were determined from the dependence of hydrolytic activity on cofactor concentration. Parameters  $K_d(\text{M2})$  obtained for V-PPase (Table 2) are essentially the same as for E-PPase. However, unlike the other bacterial PPases, inhibition of V-PPase activity was not observed up to 50 mM  $\text{Mg}^{2+}$  or 300  $\mu\text{M}$   $\text{Mn}^{2+}$  (Fig. 1). This fact might indicate the significant loss of the affinity of V-PPase for the metal ion at M4. Alternatively, occupation of this site might have no effect on the enzyme activity.

Another notable feature of V-PPase is that the pH optimum of its hydrolytic activity is shifted to more alkaline range compared to E-PPase (Fig. 2). Despite the almost total identity of amino acid residues of their active sites, the values of  $\text{p}K_{\text{ESH}}$  and  $\text{p}K_{\text{EH}}$  are surprisingly different for these two enzymes (Table 3). The only residue of the active site not identical in the two PPases is Ser99 (in E-PPase, Ala99). A new functional group occurs in the active site of V-PPase due to this replacement. Its possible connection with the change in pH profile is discussed below.

**Table 2.** Dissociation constants of *V. cholerae* and *E. coli* PPases complexed with  $\text{Mg}^{2+}$  or  $\text{Mn}^{2+}$

Parameter	V-PPase		E-PPase*	
	$\text{Mg}^{2+}$	$\text{Mn}^{2+}$	$\text{Mg}^{2+}$	$\text{Mn}^{2+}$
$K_d(\text{M2})$ , $\mu\text{M}$	$270 \pm 30$	$12 \pm 4$	$200 \pm 40$	$45 \pm 20$
$K_d(\text{M4})$ , mM	$> 50$	$> 1000$	$16 \pm 2$	$29 \pm 5$
$A_0$ , U/mg	$320 \pm 8$	$130 \pm 7$	$594 \pm 15$	$1100 \pm 50$

\* Data for E-PPase are from [13] ( $\text{Mg}^{2+}$ ) or [21] ( $\text{Mn}^{2+}$ ).

**Table 3.** The pH-independent parameters of MgPP<sub>i</sub> hydrolysis by PPases from *V. cholerae* and *E. coli*

Parameter	V-PPase	E-PPase [13]
$pK_{ESH_2}$	$7.8 \pm 0.1$	$7.6 \pm 0.3$
$pK_{ESH}$	$10.3 \pm 0.1$	$8.9 \pm 0.2$
$k_{cat}, \text{sec}^{-1}$	$170 \pm 6$	$390 \pm 80$
$pK_{EH_2}$	$7.9 \pm 0.1$	$7.7 \pm 0.8$
$pK_{EH}$	$9.7 \pm 0.1$	$8.7 \pm 0.6$
$k_{cat}/K_m, \text{sec}^{-1} \cdot \mu\text{M}^{-1}$	$26 \pm 3$	$3040 \pm 800$
$K_m, \mu\text{M}$	$6.5 \pm 0.8$	$0.13 \pm 0.06$

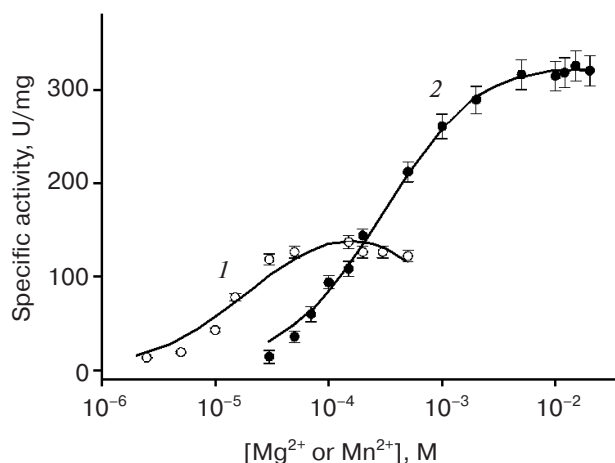
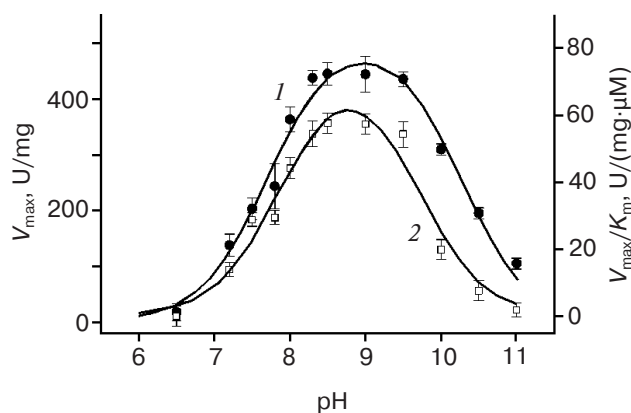
Hydrolytic activity of V-PPase was also studied as a function of concentration of NaCl, KCl, or NH<sub>4</sub>Cl. This enzyme in all three cases retained measurable activity up to 0.7–0.8 M salt. Inhibition constants were  $210 \pm 50$ ,  $150 \pm 30$ , and  $110 \pm 20$  mM for NaCl, KCl, and NH<sub>4</sub>Cl, respectively. The similarity of the values obtained for all three chlorides indicates that the enzyme is inhibited due to the elevation of ionic strength rather than the specific effects of these cations. This finding reveals another difference between V-PPase and E-PPase, since the second enzyme is specifically inhibited by Na<sup>+</sup> with  $K_i$  of about 5 mM (unpublished data). The high stability of V-PPase in solutions of high ionic strength is a noteworthy feature, which appears to be a result of evolutionary adaptation of the proteins of *V. cholerae* to a high osmolarity of its natural habitat. To determine the possible ways of osmoadaptation of PPase, we compared crystal structures of E-PPase and V-PPase and analyzed the distribution of amino acid residues not identical in their sequences.

**Comparative analysis of crystal structures of PPases from *V. cholerae* and *E. coli*.** In this work, we obtained and refined a crystal structure of V-PPase in the apo-form. The structure was solved by molecular replacement using the structure of *E. coli* pyrophosphatase as a reference model (PDB ID 1auu [16]). The final value of  $R$ -factor was 19.7%,  $R_{free}$  24.8%, the estimated standard deviation of atomic coordinates 0.25 Å. A total of 91.3% of the amino acid residues were located in the most favorable region of the Ramachandran plot, 8.4% in the additional allowed region, and 0.3% in the generously allowed region.

Amino acid sequences of family I PPases from *V. cholerae* and *E. coli* have the same length of 175 residues of which 28 are different (Fig. 3). Analysis of the crystal structure of V-PPase shows that only six of these different residues are located in the functionally significant regions: Ser99 (in E-PPase, Ala), Ala47 (Thr), Pro48

(Ala), Ile80 (Gln), Arg140 (His), and Glu143 (Asp). Only Ser99 is located in the active site.

**Active site.** Positions of the active site residues in the two PPases are shown in Fig. 4. To illustrate the location of Ser99 with respect to substrate molecule and metal cofactor ions, the structure of a metal-free form of V-PPase is superimposed on the structure of catalytically competent enzyme–substrate complex of E-PPase 2auu [16]. It can be seen that the homologous residue Ala99 in E-PPase is situated close to site M3 where a substrate metal ion is bound. This Mg<sup>2+</sup> is liganded by the neighboring residues Asp97 and Asp102. The carboxylic group of Asp102 also coordinates another Mg<sup>2+</sup> in activator site M1. The O<sub>γ</sub> atom of Ser99 in the observed structure of apo-V-PPase is too far from the expected positions of sites M1 and M3 to make contacts with either of these

**Fig. 1.** Hydrolysis of PP<sub>i</sub> by V-PPase as a function of Mn<sup>2+</sup> (1) or Mg<sup>2+</sup> (2) concentration. PPase was assayed in 50 mM Tris-HCl, pH 7.5, at 50 μM MgPP<sub>i</sub> or 20 μM MnPP<sub>i</sub>. Lines are the best fit to Eq. (2).**Fig. 2.** The pH dependence of kinetic parameters of MgPP<sub>i</sub> hydrolysis by V-PPase at 5 mM Mg<sup>2+</sup>. Parameters shown are  $V_{max}$  (1, left) and  $V_{max}/K_m$  (2, right).



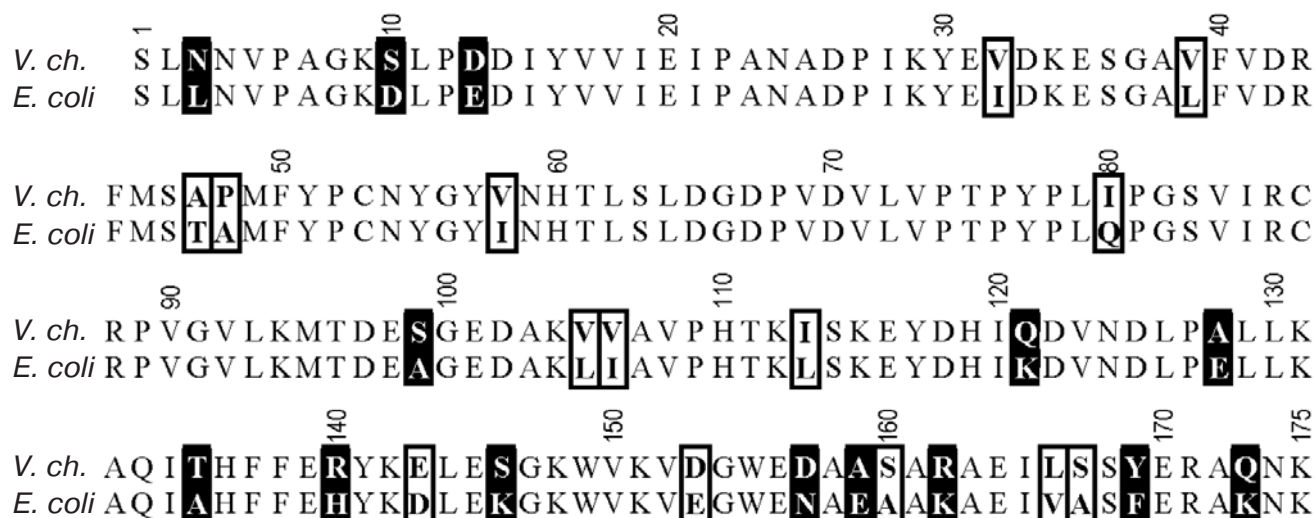


**Fig. 3.** Alignment of amino acid sequences of family I PPases from *V. cholerae* and *E. coli*. Framed are the substitutions that do not result in significant changes in the positions of side chains according to a superposition of crystal structures. Shaded in black are the substitutions that do result in significant changes of position or contacts as discussed in the text.

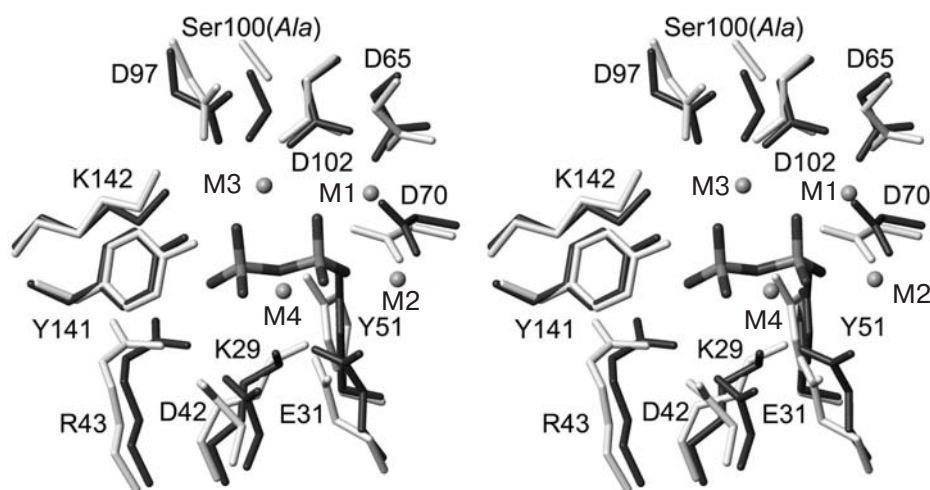


**Fig. 4.** Stereo view of active site residues. Superposition is shown of the  $C_{\alpha}$  atoms of the structures of V-PPase (apo-form; dark gray) and E-PPase (complexed with  $Mg^{2+}$ ,  $F^{-}$ , and pyrophosphate; light gray). Metal binding sites in E-PPase are indicated as M1–M4.

metal ions. However, it is likely that binding  $Mg^{2+}$  in the holo-form of V-PPase brings the OH group of Ser99 into closer proximity to M3.

Replacement of Ala99 with Ser in V-PPase might be a cause of the change in  $pK_a$  of a catalytic group of the free enzyme and enzyme–substrate complex observed in kinetic experiments ( $pK_{EH}$  and  $pK_{ESH}$ , Table 3). In the structure of apo-V-PPase, oxygen atom  $O_{\gamma}$  of Ser99 is H-bonded to a carboxylic group of Glu98, a conserved residue in the active site, which appears to be essential for the functioning of PPase, although its role remains unclear. This H-bonding might cause a difference in local distribution of electrical charges in the active site and

consequent change in  $pK_a$ . Another possible explanation is that Ser99 might be involved, directly or indirectly, in binding metal cofactor ions at sites M1 and/or M3. These metal ions and their protein ligands might partly define the values of  $pK_a$  of catalytic groups, so it is not unlikely that a change in cofactor binding might be responsible for the observed change in  $pK_a$ . The question cannot be answered here since the exact nature of the ionizable groups of soluble PPases corresponding to  $pK_{EH}$  and  $pK_{ESH}$  is still unknown.

*Intersubunit contacts and stability of hexameric V-PPase.* Five of the amino acid residues not identical in the sequences of the two enzymes are involved in E-

PPase in the formation of a hexameric structure. Gln80 forms a contact between subunits within the same trimer; Thr47, Ala48, His140, and Asp143 form the contacts between two symmetry related trimers. According to the analysis of intersubunit interfaces in V-PPase, substitutions of Gln80 with Ile, Thr47 with Ala, and Ala48 with Pro do not destroy these contacts (Table 4) since only their peptide groups were involved in the contact formation. However, substitution of His140 with Arg causes a structural difference between E-PPase and V-PPase, the consequence of which is a significant tightening of intersubunit interactions in V-PPase (Table 4 and Fig. 5a). In E-PPase, Asp143 and His140 play a major role in maintaining the stable hexameric structure. The carboxylic group of Asp143 forms an ion pair with positively charged His136 from the symmetry related subunit of the other trimer. Mutagenesis study shows that this ion pair controls stability of hexameric E-PPase at neutral pH [20]. Another histidine residue, His140, does not form direct contacts with the adjacent subunit but, being H-bonded to residues His136 and Asp143 from the same subunit, plays a key role in keeping the imidazole group of His136 positively charged [20]. In the structure of V-PPase, corresponding residues appear to be even more important part of intersubunit interaction. The carboxylic group of Glu143, like in the structure of E-PPase, forms an ion pair with His136. However, in addition to that, Glu143 in V-PPase forms a new ion pair with the guanidine group of Arg140 from the symmetry related subunit (Fig. 5b). This interaction is bidentate. The planes of guanidine groups of two Arg140 from the contacting subunits are almost parallel and their C<sub>z</sub> atoms are only 3.9 Å apart, which is indicative of these residues being in stacking or another similar kind of interaction between their coupled systems of  $\pi$ -electrons. Due to this tight contact, symmetry related trimers in V-PPase are closer to each other than in E-PPase. Therefore, the contact between trimers

**Table 4.** Intersubunit interactions (ion pairs and H-bonds) in hexameric V-PPase and E-PPase based on their crystal structures

V-PPase	E-PPase
Inside trimers	
Tyr30 OH—Ile80 NH	Tyr30 OH—Gln80 NH
Ser36 OH—Ser1 O <sub>γ</sub>	Ser36 OH—Ser1 O <sub>γ</sub>
Leu39 O—Val84 NH	Leu39 O—Val84 NH
Val41 NH—Val84 O	Val41 NH—Val84 O
Phe44 NH—Leu113 O	Phe44 NH—Leu113 O
Symmetry mirrored pairs	Symmetry mirrored pairs
Between trimers	
Asn24 N <sub>δ</sub> 2—Asp26 O <sub>δ</sub> 1	Asn24 N <sub>δ</sub> 2—Asp26 O <sub>δ</sub> 1
Ser46 O—Gln133 N <sub>ε</sub> 2	Ser46 O—Gln133 N <sub>ε</sub> 2
Pro48 O—Phe50 NH	Ala48 O—Phe50 NH
<b>His136 NH2—Glu143 O<sub>ε</sub>1</b>	<b>His136 N<sub>ε</sub>2—Asp143 O<sub>δ</sub>2</b>
<b>Arg140 N<sub>ε</sub>—Glu143 O<sub>ε</sub>1</b>	Symmetry mirrored pairs
<b>Arg140 NH2—Glu143 O<sub>ε</sub>2</b>	
Symmetry mirrored pairs	

Note: Pairs of atoms are listed with interatomic distances less than 3.1 Å. Ion pairs are given in bold.

in V-PPase is expected to be more stable than in E-PPase and the hexameric V-PPase to dissociate less readily.

Velocity sedimentation experiments show that active V-PPase functions as a hexamer, like the other

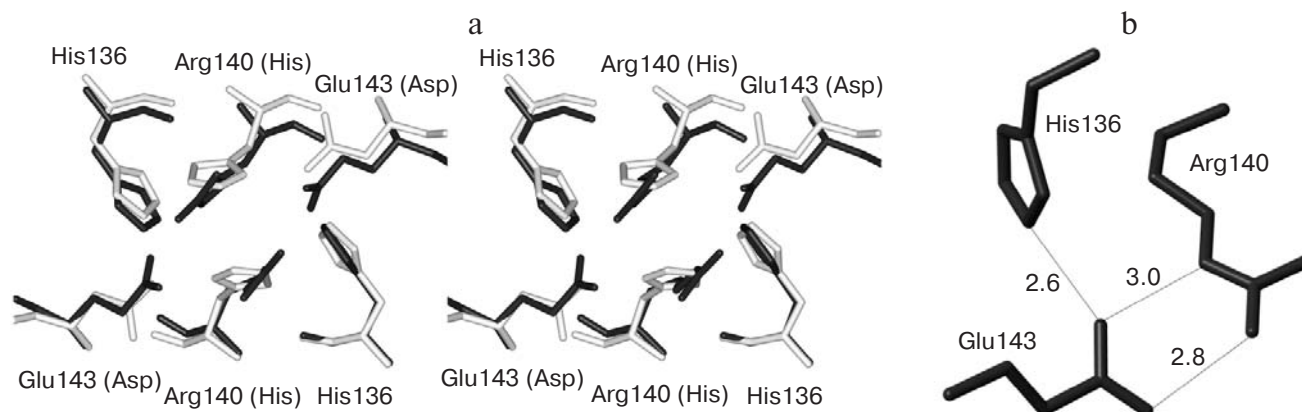


**Fig. 5.** Residues of intersubunit interface that are not identical in V-PPase and E-PPase. a) Superposition of C $\alpha$  atoms of structures of V-PPase (dark gray) and E-PPase (light gray). E-PPase residues are in parentheses. b) Interactions in V-PPase between the carboxylic group of Glu143 and residues of a symmetry related subunit His136 and Arg140. Interatomic distances are shown (Å).

**Table 5.** Sedimentation coefficients of *V. cholerae* PPase

Conditions	$s_{20}^w$ , S
50 mM Hepes, pH 7.5	$7.5 \pm 0.3$
0.1 M Mes, pH 5.3	$6.3 \pm 0.3$
0.1 M Mes, pH 4.5	$6.4 \pm 0.3$
0.1 M Mes, pH 3.1	$6.5 \pm 0.3$ (hexamer) $3.8 \pm 0.3$ (trimer)

known bacterial PPases of family I. The sedimentation coefficient of V-PPase corresponds to a hexameric molecule ( $s_{20}^w = 6.4$  S) even at pH < 5 where E-PPase is known to dissociate to trimers (Table 5). Trace amounts of trimeric V-PPase ( $s_{20}^w = 3.8$  S) were observed only at pH as low as 3.1. Similarly to E-PPase, acid pH-induced dissociation of hexameric V-PPase to trimers appears to be caused by protonation of Glu143 and consequent melting of ion pairs formed by this residue, which control stability of a hexamer. However, in the case of V-PPase, in addition to the pair Glu143–His136, there is an extra ion contact Glu143–Arg140, which could explain why Glu143 in this enzyme has a lower  $pK_a$  and the hexamer is more stable at pH below 5 than in the case of E-PPase.

To determine the  $pK_a$  of Glu143, samples of V-PPase of the same concentration were incubated at various fixed pH values for 4–5 h followed by the measurement of hydrolytic activity of the samples in the standard PPase assay. As a result of incubation at low pH, there was a loss of PPase activity to some constant level, which did not change over the next 5–10 h. The level of residual activity depended on pH, this dependence indicating the  $pK_a$  of the group controlling dissociation, i.e. Glu143. Acid pH-induced inhibition of PPase was reversible to a significant degree. PPase activity of a sample incubated at low pH could be partly restored by its incubation in a solution of optimal pH (7.5–9.0). Different degree of reactivation could be obtained depending on the pH of incubation mixture and enzyme concentration. For instance, 1  $\mu$ M enzyme incubated at pH 4.4 restored 70% of its original activity after its dilution 1 : 10 with buffer of pH 9.0. According to the results of velocity sedimentation experiments, in the solution of 20  $\mu$ M V-PPase at pH 3.1 the most populated oligomeric form was a hexamer, and therefore denaturation did not occur under these conditions. Taken together, these results demonstrate that acid pH-induced inhibition of PPase is caused mostly by its reversible dissociation rather than denaturation, and therefore the equilibrium parameters can be determined from the observed dependence. On the other hand, a contribution of some irreversible process in the inhibition becomes notable at pH below 4.0. It can be partial denaturation or irreversible conformational change of dissociated subunits that makes it impossible to restore a native hexamer. Due to this contribution, the value of  $pK_a$  obtained from the experimental data is supposed to be slightly higher than its actual value and can be regarded as the upper limit of the actual  $pK_a$  of Glu143.

As we expected, the value obtained from pH dependence ( $pK_a = 4.4 \pm 0.2$ ) is significantly lower than the value obtained earlier for the Asp–His pairs in PPases from *E. coli* and *M. tuberculosis* ( $pK_a = 5.6$  and  $5.4$ , respectively [11, 20]). The fact that  $pK_a$  of Glu143 in V-PPase is lower than the  $pK_a$  of the analogous residues of the other hexameric PPases might indicate a greater contribution of ionic interactions in the total oligomeric stability of this enzyme. It should also be noted that, unlike E-PPase, residual hydrolytic activity of V-PPase after incubation at acid pH approaches zero level, whereas in the case of E-PPase acid dissociation resulted in formation of trimers with relative activity of 10% of the original activity of the hexameric form. Formation of an oligomeric form with zero activity upon acid dissociation was earlier observed for Mt-PPase. In this enzyme, due to unique structure of its intersubunit contacts and consequent increase in their ionic character, acid pH-induced dissociation of hexamers resulted in inactive monomers [11]. Similarly, an increased contribution of ionic interactions between subunits of V-PPase appears to cause the cooperative dissociation of its hexamers at low pH to inactive monomers.

**Stabilization of a globular structure.** Four substitutions in V-PPase compared to E-PPase (Leu3 with Asn, Ala135 with Thr, Phe169 with Tyr, and Lys173 with Gln) result in the formation of additional contacts between the elements of secondary structure. The side chain of Asn3 is H-bonded to the oxygen atoms of peptide groups of Lys34 and Glu35, thus bridging a short N-terminal helix  $3_{10}$  with a loop connecting  $\beta$ -strands  $\beta 2$  and  $\beta 3$ . The OH group of Thr135 is H-bonded to the peptide oxygen atom of Lys131 and  $N_{\epsilon}1$  atom of Trp155 bridging  $\alpha$ -helix  $\alpha 1$  with  $\beta$ -strand  $\beta 8$ . The side chain of Gln173 is H-bonded to the OH group of Tyr169 and the peptide oxygen atom of His60 bridging a C-terminal  $\alpha$ -helix with a  $\beta$ -turn connecting  $\beta 4$  and  $\beta 5$ . Substitutions of Leu3 with Asn and Lys173 (a third residue from the C-terminus) with Gln provide tighter attachment of both N- and C-terminal regions to the protein body. Along with the replacement of His140 with Arg discussed above, these substitutions might promote the stability of PPase at high salt concentrations and thus might occur as a result of evolutionary adaptation of *V. cholerae* to high osmolarity of estuarine waters.

According to literature data [5, 6], a common way of osmoadaptation of proteins of halophilic organisms is maintaining of numerous binding sites for monovalent cations. These cations stabilize protein structure by keeping it highly solvated with water molecules. Neither  $Na^+$  nor  $K^+$  was observed in the structure of V-PPase since in



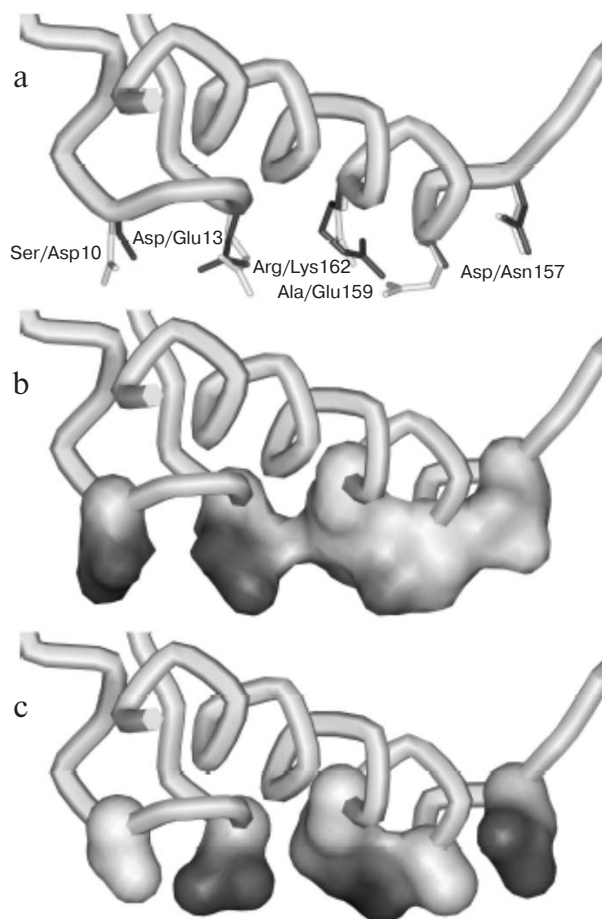


**Fig. 6.** Solvent-exposed residues that are not identical in V-PPase and E-PPase. a) Secondary structure elements (C-terminal  $\alpha$ -helix, and a hairpin connecting N-terminal  $\alpha$ -helix with  $\beta$ 1) and side chains of the variable residues forming a recognition strand (V-PPase, dark gray; E-PPase, light gray). b, c) Molecular surface of the same region in E-PPase (b) and V-PPase (c) colored by electrostatic potential (dark, charged; light, uncharged).

the course of its crystallization nonionic agents were used as precipitants.

Another well-known structural feature of halophilic proteins is an excess of acidic over basic residues, especially on the protein surface where they help maintain a highly ordered solvation shell [4-7]. However, no increase in acidic character is observed in V-PPase compared to its non-halophilic counterpart. The calculated value of  $pI$  for V-PPase is 4.9, which is essentially the same as for E-PPase (5.0). A comparison of the solvent-exposed amino acid residues different in the two enzymes reveals substitutions of both kind, i.e. yielding either negative (for example, Asn157 in E-PPase versus Asp in V-PPase, Lys121 versus Gln) or positive (Glu128 versus Ala, Asp10 versus Ser) change of the net charge. Analysis of non-identical residues on the protein surface shows an interesting structural feature. Five of these residues sit along a straight line. In E-PPase, their side chains form a charged

strand on the surface of a hexamer (Fig. 6a). Two of them (Asp10, Glu13) are extended from the  $\beta$ -turn immediately following the N-terminal helix, and another three (Asn157, Glu159, Lys162) are extended from the C-terminal  $\alpha$ -helix. In the sequence of V-PPase, two of three carboxylic groups are substituted resulting in the loss of negative charges, in the spatial structure one of them being replaced with positively charged arginine (Arg162). The fourth residue (Asn157) is replaced with Asp, also with the change of a charge. This distinct pattern of highly variable residues might play a role in the recognition of potential protein targets of PPase, possibly interacting with the functional groups residing along an  $\alpha$ -helix of a target protein. If this supposition is correct, the difference between recognition patterns found here for PPases from *E. coli* and *V. cholerae* (Fig. 6, b and c) appears to mirror the difference between the corresponding patterns in their protein partners.

The authors thank Prof. R. Lahti (Turku University, Finland) for kindly providing the plasmid of family I PPase from *V. cholerae* and Prof. H. Bartunik (Max Planck Unit, Hamburg, Germany) for providing the opportunity to collect diffraction data.

This work was financially supported by the Russian Foundation for Basic Research (grant No. 06-04-49127) and Russian Federal Space Agency (Roskosmos).

## REFERENCES

1. Pflughoeft, K. J., Kierek, K., and Watnick, P. I. (2003) *Appl. Environ. Microbiol.*, **69**, 5919-5927.
2. Huq, A., West, P. A., Small, E. B., Huq, M. I., and Colwell, R. R. (1984) *Appl. Environ. Microbiol.*, **48**, 420-424.
3. Roesser, M., and Muller, V. (2001) *Environ. Microbiol.*, **3**, 743-754.
4. Dym, O., Mevarech, M., and Sussman, J. L. (1995) *Science*, **267**, 1344-1346.
5. Tokunaga, H., Arakawa, T., and Tokunaga, M. (2008) *Protein Sci.*, **17**, 1603-1610.
6. Manikandan, K., Bhardwaj, A., Gupta, N., Lokanath, N. K., Ghosh, A., Reddy, V. S., and Ramakumar, S. (2006) *Protein Sci.*, **15**, 1951-1960.
7. Frolow, F., Harel, M., Sussman, J. L., Mevarech, M., and Shoham, M. (1996) *Nat. Struct. Biol.*, **3**, 452-458.
8. Heinonen, J. K. (2001) *Biological Role of Inorganic Pyrophosphate*, Kluwer Academic Publishers, Inc., Boston.
9. Heidelberg, J. F., Eisen, J. A., Nelson, W. C., Clayton, R. A., Gwinn, M. L., Dodson, R. J., Haft, D. H., Hickey, E. K., Peterson, J. D., Umayam, L. A., Gill, S. R., Nelson, K. E., Read, T. D., Tettelin, H., Richardson, D. L., Ermolaeva, M. D., Vamathevan, J. J., Bass, S., Qin, H., and Fraser, C. M. (2000) *Nature*, **406**, 477-483.
10. Salminen, A., Ilias, M., Belogurov, G. A., Baykov, A. A., Lahti, R., and Young, T. (2006) *Biochemistry (Moscow)*, **71**, 978-982.
11. Rodina, E. V., Vainonen, L. P., Vorobyeva, N. N., Kurilova, S. A., Sitnik, T. S., and Nazarova, T. I. (2008) *Biochemistry (Moscow)*, **73**, 897-905.



12. Baykov, A. A., and Avaeva, S. M. (1981) *Anal. Biochem.*, **116**, 1-4.
13. Rodina, E. V., Vainonen, Y. P., Vorobyeva, N. N., Kurilova, S. A., Nazarova, T. I., and Avaeva, S. M. (2001) *Eur. J. Biochem.*, **268**, 3851-3857.
14. Otwinowski, Z., and Minor, W. (1997) *Meth. Enzymol.*, **276**, 307-326.
15. Vagin, A. A., and Teplyakov, A. (1997) *J. Appl. Cryst.*, **30**, 1022-1025.
16. Samygina, V. R., Moiseev, V. M., Rodina, E. V., Vorobyeva, N. N., Popov, A. N., Kurilova, S. A., Nazarova, T. I., Avaeva, S. M., and Bartunik, H. D. (2007) *J. Mol. Biol.*, **366**, 1305-1317.
17. Murshudov, G. N., Vagin, A. A., and Dodson, E. J. (1997) *Acta Crystallogr. Sect. D*, **53**, 240-255.
18. Emsley, P., and Cowtan, K. (2004) *Acta Crystallogr. Sect. D*, **60**, 2126-2132.
19. Gasteiger, E., Gattiker, A., Hoogland, C., Ivanyi, I., Appel, R. D., and Bairoch, A. (2003) *Nucleic Acids Res.*, **31**, 3784-3788.
20. Velichko, I. S., Mikalahti, K., Kasho, V. N., Dudarenkov, V. Y., Lahti, R., and Baykov, A. A. (1998) *Biochemistry*, **37**, 734-740.
21. Vainonen, Ju. P., Rodina, E. V., Vorobyeva, N. N., Kurilova, S. A., Nazarova, T. I., and Avaeva, S. M. (2001) *Rus. Chem. Bul.*, **50**, 1877-1884.